



## Article

# Experimental Assessment on Exploiting Low Carbon Ethanol Fuel in a Light-Duty Dual-Fuel Compression Ignition Engine

Carlo Beatrice <sup>1</sup>, Ingemar Denbratt <sup>2</sup>, Gabriele Di Blasio <sup>1,\*</sup> , Giuseppe Di Luca <sup>1</sup>, Roberto Ianniello <sup>1</sup>  and Michael Saccullo <sup>2</sup>

<sup>1</sup> Istituto Motori-Consiglio Nazionale delle Ricerche, 80125 Napoli NA, Italy; c.beatrice@im.cnr.it (C.B.); g.diluca@im.cnr.it (G.D.L.); r.ianniello@im.cnr.it (R.I.)

<sup>2</sup> Department of Applied Mechanics, Chalmers University of Technology, 412 96 Göteborg, Sweden; denbratt@chalmers.se (I.D.); michael.saccullo@chalmers.se (M.S.)

\* Correspondence: gabriele.diblasio@cnr.it

Received: 11 September 2020; Accepted: 13 October 2020; Published: 15 October 2020



**Abstract:** Compression ignition (CI) engines are widely used in modern society, but they are also recognized as a significative source of harmful and human hazard emissions such as particulate matter (PM) and nitrogen oxides (NO<sub>x</sub>). Moreover, the combustion of fossil fuels is related to the growing amount of greenhouse gas (GHG) emissions, such as carbon dioxide (CO<sub>2</sub>). Stringent emission regulatory programs, the transition to cleaner and more advanced powertrains and the use of lower carbon fuels are driving forces for the improvement of diesel engines in terms of overall efficiency and engine-out emissions. Ethanol, a light alcohol and lower carbon fuel, is a promising alternative fuel applicable in the dual-fuel (DF) combustion mode to mitigate CO<sub>2</sub> and also engine-out PM emissions. In this context, this work aims to assess the maximum fuel substitution ratio (FSR) and the impact on CO<sub>2</sub> and PM emissions of different nozzle holes number injectors, 7 and 9, in the DF operating mode. The analysis was conducted within engine working constraints and considered the influence on maximum FSR of calibration parameters, such as combustion phasing, rail pressure, injection pattern and exhaust gas recirculation (EGR). The experimental tests were carried out on a single-cylinder light-duty CI engine with ethanol introduced via port fuel injection (PFI) and direct injection of diesel in two operating points, 1500 and 2000 rpm and at 5 and 8 bar of brake mean effective pressure (BMEP), respectively. Noise and the coefficient of variation in indicated mean effective pressure (COV<sub>IMEP</sub>) limits have been chosen as practical constraints. In particular, the experimental analysis assesses for each parameter or their combination the highest ethanol fraction that can be injected. To discriminate the effect on ethanol fraction and the combustion process of each parameter, a one-at-a-time-factor approach was used. The results show that, in both operating points, the EGR reduces the maximum ethanol fraction injectable; nevertheless, the ethanol addition leads to outstanding improvement in terms of engine-out PM. The adoption of a 9 hole diesel injector, for lower load, allows reaching a higher fraction of ethanol in all test conditions with an improvement in combustion noise, on average 3 dBA, while near-zero PM emissions and a reduction can be noticed, on the average of 1 g/kWh, and CO<sub>2</sub> compared with the fewer nozzle holes case. Increasing the load insensitivity to different holes number was observed.

**Keywords:** dual-fuel; compression ignition engine; ethanol; nozzle-hole number; soot emissions

## 1. Introduction

The International Energy Outlook 2019 shows that the fuel demand is expected to rise over the next three decades, and the fossil fuel share is estimated at 80% of energy use in 2050 [1]. Besides,

the transition to a more advanced form of propulsion (such as hybrid cars, electric vehicles, fuel cells, etc.) developed for fuel economy improvement and reduction in exhaust emissions is very far to be complete. As a result, stringent emission legislation and higher oil prices push world Original Equipment Manufacturers (OEMs) to investigate more efficient engines. Compression ignition (CI) engines, due its efficiency, robustness, flexibility and low operation cost, are widely used in modern society in many operative fields such as passenger vehicles, industrial or agricultural equipment, or as stationary sources of energy. The main concern using diesel engines is related to the drawback of higher emissions of particulates matter (PM) and nitrogen oxides (NOx). The typical diesel PM–NOx trade-off makes it difficult to control these pollutant emissions simultaneously [2]. In this context, to meet the more stringent emissions directions [3] (setting new CO<sub>2</sub> emission standards for cars and vans, Euro 6 emissions standard regulates particulate and gaseous emissions), modern diesel engines are equipped with complex and costly after-treatment systems, to reduce PM emissions and selective catalytic reduction that injects ammonia or urea into exhaust gases stream to reduce NOx [4]. A solution to reduce costs can be reducing the engine-out emissions directly through advanced combustion process like low-temperature combustion (LTC) strategies. These approaches are considered a promising way to improve the efficiency of CI engines while reducing NOx and PM emissions simultaneously. In LTC, the combustion temperature is kept below the soot-forming region, and the lower temperature allows one to avoid thermal NOx formation [5]. Several LTC concepts like homogenous charge compression ignition (HCCI) and premixed charge compression ignition (PCCI), among others, have been suggested to achieve overall lower engine-out emissions [6]. LTC in a diesel-fuelled engine requires the production of a lean premixed charge to ensure a long ignition delay (ID) to enhance the charge homogeneity. Several strategies can be used to delay ignition such as early injection timing or high rate of exhaust gas recirculation (EGR) [7] allowing a simultaneous near-zero NOx and PM emissions [8] at the cost of high levels of unburned HC and CO [9].

A strategic way to achieve this purpose is using alternative and cleaner fuels [10]. Among them, ethanol is considered to be one of the most promising alternative fuels in diesel engines, which can significantly contribute to the reduction of particulate emissions at the exhaust [11]. It can be produced by direct fermenting of sugars, including sugarcane, sugar beet, sorghum, whey and molasses with yeast, from lignocellulosic materials, including woody materials, straws, agricultural waste and crop residues and catalytic hydration of ethylene [12]. Recently the ethanol production from microalgae gains attention due to their easy process to be converted in monosaccharides for biofuels production, to their high growth rate and short harvesting cycle [13]. For the aforementioned reasons, ethanol can be considered as a biofuel. The Kyoto protocol treats biofuels as carbon neutral because CO<sub>2</sub> emission for biofuel combustion is balanced out by absorbed CO<sub>2</sub> during the growth of the plants for its production [14]. In addition, the ethanol production from microalgae can be integrated into a circular sustainable process to generate clean water and energy reaching CO<sub>2</sub> fixation, and oxygen release [15]. There are several techniques involving ethanol–diesel in dual-fuel (DF) operation, and each concept comes with its upsides and downsides [16]. The simplest method is to add ethanol to the conventional diesel fuel and injecting the blend directly into the cylinder through the conventional diesel injector. The alcohol–diesel blends help to reduce engine emissions without significant impacts on engine performance. The main disadvantage is that the fuel substitution ratio (FSR) cannot be changed instantaneously and the ethanol fraction is limited due to its poor ignitibility and miscibility (this can be partly alleviated by emulsifying the mixture) [17]. Due to its low cetane rating (<10), ethanol also represents an interesting solution to be used as injected fuel via port fuel injection (PFI). When injecting the diesel and alcohol fuel separately into the cylinder, the substitution ratio can be changed faster than the previous case, and more diesel can be substituted with alcohol fuel than the blend case [18]. The main technical issue related to this concept is the use of two separate injectors leading to a more complex hardware and electronic systems conversion; nevertheless, the engine intake is generally easily accessible. This DF concept poses an upper limit for fuels substitution ratio due to knocking and

ringing issues associated with a higher degree of premixed combustion in combination with a high compression ratio typical of a diesel engine [19].

In [20], the authors summarized a significant quantity of literature related to the alcohol fumigation concept in the dual-fuel combustion mode. The findings reported are related to the effect of alcohol fumigation on engine characteristics, such as brake specific fuel consumption or thermal efficiency, and gaseous and PM emissions. In general, the reported results show that efficiency decreases at low loads; small increases can be observed for medium and high loads. Regarding NO<sub>x</sub> emissions, their reduction is proportional to the alcohol fraction, and they are significantly affected by engine loads. A reduction of PM emissions is also reported due to the low PM tendency of alcohol fuel due to the oxygen content. In this way, the traditional NO<sub>x</sub>-PM trade-off is circumvented. In all findings reported in [16], CO and HC emissions increase due to lower mean in-cylinder temperature related to the “cooling” effect of the alcohol fuel. The increase of HC emissions is also related to the quenching phenomenon and mixture trapped into the crevices. Many other authors study the effect of ethanol in the DF mode adopting EGR, e.g., Pedrozo et al. [21] observed that high fraction of ethanol leads to a reduction of NO<sub>x</sub> and employing EGR further improvements are observed with no adverse effect on engine efficiency. Asad et al. [22] found that the use of ethanol in the DF mode with a high rate of EGR and a retarded single injection strategy lead to ultra-low NO<sub>x</sub> and PM emissions at the cost of elevated HC and CO emissions.

Among the extensive literature on ethanol dual-fuel engines, this study provides new findings to the technical literature on the maximum ethanol fraction as a function of the nozzle hole numbers and its influence on the combustion behavior in the DF mode and emissions, particularly greenhouse gas (GHG). The analysis was conducted because of the combustion process in the DF mode starts from high reactivity zones in the combustion chamber, and the nozzle hole number can influence the number of these zones. To achieve this goal, the maximum fuel substitution ratio (FSR) is evaluated in a dual-fuel (DF) combustion mode by means a one-factor-at-a-time parametric analysis to discriminate the effects of the calibration parameters (combustion phasing CA<sub>50</sub>, rail pressure, injection strategy, and EGR). With the appropriate calibration, the influence of injector nozzle holes number on maximum FSR, engine combustion indicators and emissions are assessed.

The experimental investigations were conducted on an Light-Duty (LD) single-cylinder diesel engine in two steady-state test points, 1500 and 2000 rpm related to low and medium engine load conditions. After the experimental setup and procedure description, in the last part of the manuscript, first is discussed how the maximum fuel substitution ratio (FSR) is influenced by the combustion phasing, rail pressure, injection pattern and exhaust gas recirculation (EGR). Then the influence of the nozzle hole number in the dual-fuel operating mode is discussed.

## 2. Materials and Methods

### 2.1. Experimental Setup and Fuels

The test campaign was performed on a single-cylinder CI research engine characterized by a combustion system derived from a Euro6 compliant four-cylinder engine, representative of current LD diesel technology. The four-cylinder head, derived from the production series, was modified to operate in single-cylinder configuration. The engine specifications are given in Table 1. The auxiliary engine systems were characterized by maximum flexibility without affecting the load conditions. The electronic control unit, National Instrument and Labview based allows the management of all the engine control parameters. This approach offers great flexibility for all operating conditions.

Table 1. Main engine characteristics.

Displaced Volume	489 (cc)
Bore × Stroke	83 × 90.4 (mm)
Compression Ratio	16
Number of Valves	4
Common Rail Injection System	2500 bar max pressure
Diesel Injector	Solenoid actuation—7 and 9 holes
Nozzle Hydraulic Flow Rate	440 (cm <sup>3</sup> /30 s)
PFI Injector (Ethanol)	Solenoid Multi-hole

The engine was modified to operate in the DF mode. Port fuel injection (PFI), typical for DF operation, was carried out through a dedicated PFI injector positioned at the intake manifold. A separate low-pressure line powered the PFI injector. Both fuels, diesel and ethanol were measured using gravimetric mass flow meters. Figure 1 shows the schematic layout of the experimental setup used in this test campaign.

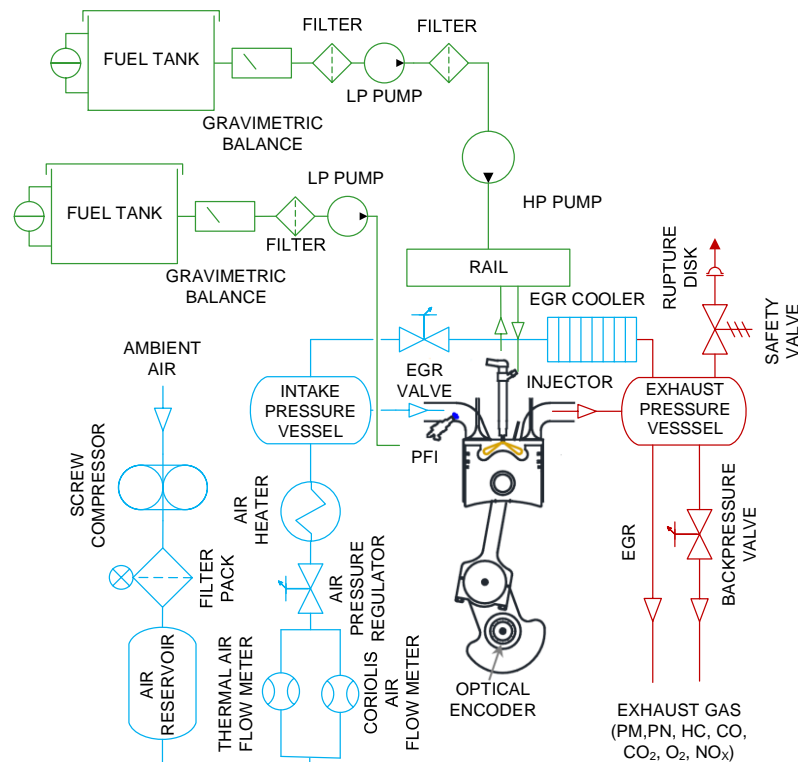


Figure 1. Experimental test cell layout.

An integrated and commercial exhaust gas analyzer (AVL CEB II) coupled to a smoke meter (AVL 415 S) was used to measure the exhaust gases and smoke emissions. The in-cylinder pressure was measured through a piezoelectric pressure sensor placed on the cylinder head in the glow plug seat [23]. The heat release rate was computed by the AVL IndiMicro<sup>®</sup> system starting from the pressure signal acquired following the first law of thermodynamics [2]. For each tested point, the in-cylinder pressure traces were averaged over 128 cycles to average cycle-to-cycle variation. Steady state tests were repeated at least three times to ensure acceptable repeatability within experimental uncertainties. Table 2 shows the fuel properties from fuels tested for the test campaign presented in this paper.

Table 2. Fuel properties [2,24].

Properties	Diesel	Ethanol
Research Octane Number (-)	-	108–109
Molar Mass (g/mol)	170	46.07
H/C (-)	1.8	3
O/C (-)	0	0.5
LHV (MJ/kg)	42.9	26.9
(A/F)s (-)	14.5	9.0
Viscosity (mPa/s)	3.91	1.36
Density (kg/m <sup>3</sup> )	837	785
Boiling Point (°C)	184–362	78
Heat of Vaporization (kJ/kg)	270	840
Specific Heat (kJ/kgK)	2.2	2.5

## 2.2. Experimental Methodology

The operating points were performed using a Euro 6 Diesel engine calibration (e.g., boost, backpressure, injection parameters, etc.) to ensure a practical parameters migration on real light-duty engine applications. The investigations were conducted at two operating points under a steady state engine speed of 1500 rpm, and 2000 rpm and 5 and 8 bar of brake mean effective pressure (BMEP) respectively. The level of premixed ethanol, quantified by the fuel substitution ratio (FSR), can be defined through the following equation:

$$FSR = \frac{m_p \cdot LHV_p}{m_p \cdot LHV_p + m_d \cdot LHV_d} \quad (1)$$

LHV<sub>p</sub> and LHV<sub>d</sub> indicate the lower heating value respectively of premixed ethanol and direct-injected diesel, while  $m_p$  and  $m_d$  their respective mass flow rate. The combustion duration is defined as the crank angle duration between CA10 and CA90, where the 10% and 90% of the total heat release occurred, respectively. The ignition delay (ID) is defined as the crank angle difference between CA10 and the start of injection (SOI). The start of direct diesel injection (SOI<sub>diesel</sub>) and the injection durations for both fuels were varied to achieve the reference combustion phasing (CA50) and BMEP values, respectively.

The first step of the test procedure consisted of an engine warm-up procedure, which was carried out in the diesel mode to reach the loads' targets. Switching to the DF mode, the quantity of diesel injected was reduced while ethanol fraction was proportionally increased to reach the maximum FSR at the same load. Ethanol fuel was injected via PFI at 5 bar at the constant start of injection (SOI<sub>ethanol</sub>), fixed at 360 deg bTDC. The intake air temperature was kept constant in all test conditions and equal to 60 °C. The experimental conditions are summarized in Table 3.

Table 3. Test conditions.

	P <sub>int</sub> (barG)	P <sub>exh</sub> (barG)	IMEP (bar)	PFI <sub>pressure</sub> (bar)	SOI <sub>ethanol</sub> (deg bTDC)	T <sub>ethanol</sub> (K)
1500 × 5	0.3	0.6	6.2	5	360	333
2000 × 8	0.6	1.0	9.2			

To achieve the maximum FSR, which was the main target of the investigation, a parametric analysis of different parameters was performed. First, a CA50 sweep was made through the SOI variation of the direct-injected diesel fuel, in the interval 4–14 CA after top dead centre (aTDC). The FSR value assessed was considered maximum when the noise limit bound to 90 dBA and a stable engine conditions quantified by a COV<sub>IMEP</sub> up to 3% were achieved. The noise level was determined through

a transfer function using the peak release rate (PRR) as input. These constraints were maintained in all experimental tests performed in this study. The FSR values assessed with CA50 variation were considered as a reference in the next sweeps.

At the operating point  $1500 \times 5$ , the experimental assessments were conducted at constant diesel injection pressure (500 bar). The influence of higher injection pressure (1000 bar) was also evaluated, adopting an only main injection strategy. Nevertheless, at lower injection pressure (500 bar) an injection pattern sweep was also analyzed in order to evaluate if a multi-injection strategy guaranteed the same engine performance of the only one. For the operating point  $2000 \times 8$ , in order to ensure an acceptable combustion stability index, a multi injection strategy was used with an injection pressure of 700 bar. Additionally, for this test point, the influence of enhanced injection pressure (1000 bar) was evaluated. It is worth highlighting that in this test point, the use of a preferable single pulse direct injection did not allow us to observe the imposed noise and  $COV_{IMEP}$  limits. To this aim, a multi-injection strategy derived from the diesel calibration settings was adopted, leading to an overall improvement of the engine performance and emissions outputs [25]. Figure 2 shows the injection patterns employed for the test campaign, and Table 4 the test matrix for both test points.

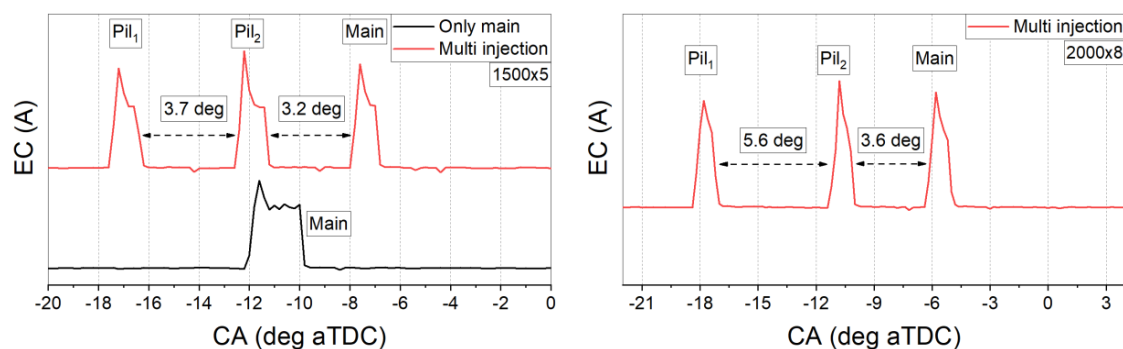


Figure 2. Injection pattern for the tested operating points.

Table 4. Engine parameters variation range sequence.

Parameters	$1500 \times 5$		$2000 \times 8$	
CA50 Range of Variation	4–14 deg		4–14 deg	
Rail Pressure	500 bar	1000 bar	700 bar	1000 bar
Injection Pulses	Main	Multi-inj.	Multi-inj.	
NOx Target (EGR)	78 ppm		120 ppm	
Nozzle (#)	7 holes	9 holes	7 holes	9 holes

### 3. Results and Discussion

In the following sections, Sections 3.1–3.4, the influence on maximum FSR engine calibration parameters (injection pressure, injection pattern, EGR) are presented. These sections explain the main effects of the calibration parameters considered on engine behavior working in the DF mode. In the last paragraph, Section 3.5, the injector nozzle hole effects on the maximum ethanol fraction that could be reached and on the GHG and PM emissions were evaluated. A comparison between dual-fuel and conventional diesel modes were discussed.

#### 3.1. Definition of Maximum FSR Function of CA50

In this section, the main results in terms of maximum FSR reached for each of the CA50 in the considered interval and for the two test points considered were discussed.

Figure 3 shows the FSR function of the CA50 for the steady state test point at 1500 rpm and 5 bar BMEP. The evaluation was conducted for various levels of combustion phasing, from 4 to 14 deg aTDC,

as shown in Table 3, with no EGR, only the main injection strategy and a diesel injection pressure of 500 bar.  $SOI_{Ethanol}$  was fixed at 360 deg bTDC<sub>firing</sub> and an injection pressure of 5 bar. To some extent this setting helped to distinguish the single effect of the CA50 variation on FSR in the DF mode keeping constant the other parameters.

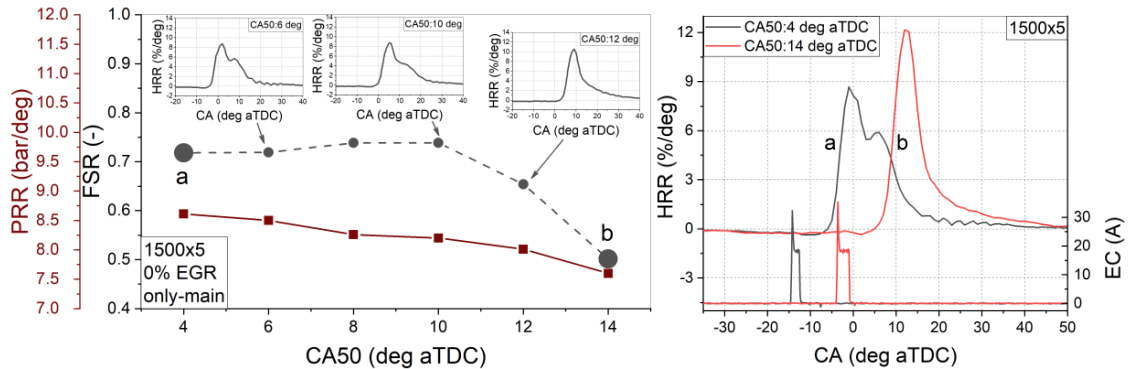


**Figure 3.** Maximum fuel substitution ratio (FSR) and pressure rise rate (PRR) function of CA50, with a single injection strategy and no exhaust gas recirculation (EGR) at  $1500 \times 5$ . Heat release rate (HRR) profiles and injection patterns at  $1500 \times 5$ , for CA50 4 (a) and 14 (b) deg after top dead centre (aTDC).

Higher values of FSR were achieved for more advanced CA50. FSR shows a flat trend (70–74%) in the range of 4–10 deg aTDC. For a higher CA50, 10–12 deg aTDC, the ethanol fraction was reduced to observe the imposed combustion noise and  $COV_{IMEP}$  limits. It was necessary to reduce the FSR to keep the pressure rise rate (PRR) constant, as shown in Figure 3.

To better characterize and understand the constraints in terms of the FSR increment, the combustion process evolutions of significant operating points, heat release rate (HRR) trends with related injection phases, are also depicted in Figure 3. At 4 deg of CA50, the combustion process showed both a premixed and diffusive combustion phases. With a diesel injection near TDC, the consequently retarded combustion phasing led to faster and prominent premixed combustion phase with a less pronounced diffusive phase as HRR profiles show. A retarded combustion phasing also led to a better air-fuel homogenization, which burns rapidly in the premixed combustion phase and consequently a shorter end of combustion phase was established. Moving to more retarded combustion phasing, the HRR pattern observed is typical of an RCCI (Reactivity Controlled Compression Ignition) combustion process [6]. With ethanol injection, the diesel fuel burned in the diffusion mode is now combusting in a mixture of ethanol/air, which burns in the premixed mode [26]. Longer combustion duration was observed, as remarked in Table 5.

**Table 5.** Combustion duration function of combustion phasing.

	1500 × 5	2000 × 8
CA50 (deg aTDC)	CA90-10 (deg)	
4	17.6	21
6	17.2	21.6
8	17.9	21.7
10	19.8	22.7
12	20.4	24.6
14	21.2	26

Figure 4 shows the FSR trend as a function of CA50 at  $2000 \times 8$ . The evaluation was conducted for the same CA50 range, ethanol injection pressure and  $SOI_{Ethanol}$  introduced in the previous case (Table 3), with no EGR and a diesel injection pressure of 700 bar. In contrast to the lower load point  $1500 \times 5$ , this test point employed a multi injection pattern to ensure acceptable combustion stability. The comparative results among combustion phasing show FSR values ranging in the interval 80–85%,

higher compared to the previous case, and its trend can be considered as constant. Further increments were not possible due to ringing and noise limitations. Furthermore, due to a lower fraction of diesel injected longer combustion duration was observed as remarked in Table 5.

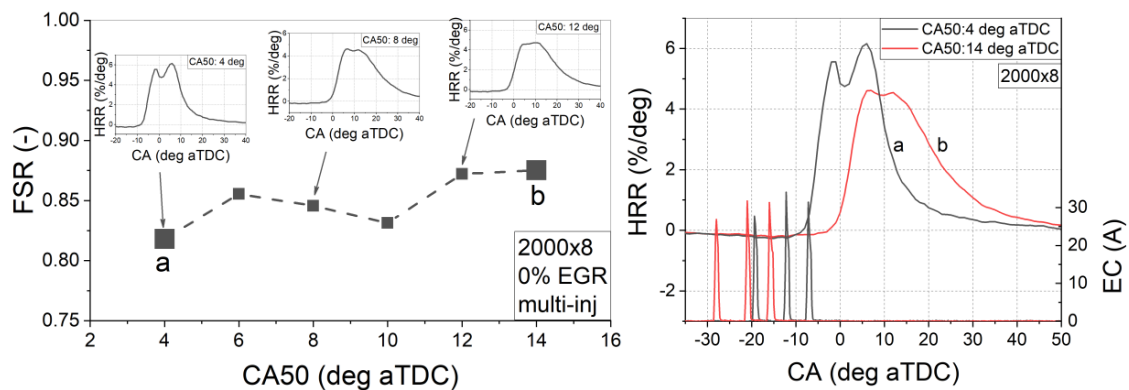


**Figure 4.** Maximum FSR function of CA50 with a multi-injection strategy, no EGR at  $2000 \times 8$ . HRR profiles and injection patterns in  $2000 \times 8$  test point at 4 (a) and 14 deg (b) aTDC.

Figure 4 compares the HRR profiles at 4 and 14 deg of CA50. As seen, for more advanced combustion phasing (4 deg) the HRR profile shows two characteristic peaks, the first one was related to the burning of the pilot diesel fuel and the second to the burning of the ethanol as the main energy carrier. HRR profiles lose the two peaks previously observed retarding combustion phase and increasing the ethanol fraction. The progressive loss of the first diesel peak was due to the high heat of vaporization of alcohol injected; hence its cooling effect became more significant on the combustion rate [27]. The HRR profile comparison indicates a transition to a premixed, homogeneous ethanol-dominated combustion [22]. Related to the previous point, the cooling effect of ethanol lowered the HRR peak.

### 3.2. Effects of Diesel Fuel Injection Pressure on FSR in the DF Mode

This section shows the experimental results on the influence of diesel injection pressure on the maximum FSR. To discriminate this effect on the FSR, an injection pressure of 1000 bar was considered, and all the other parameters were kept constant. It is worth highlighting that a different injection strategy was used in the two operating points considered. Furthermore, the maximum FSR assessed in the previous section was used as a reference.

As seen in Figure 5, in  $1500 \times 5$  test point despite a higher injection pressure, the FSR trend was similar to the reference one over the CA50 range considered. In terms of the combustion process, as HRR profiles show, the higher diesel injection pressure seemed not to produce relevant changes. Important differences can be noticed for 14 deg aTDC, where a lower peak in the HRR trend was observed due to a slight increase in the ethanol fraction. It is also noticed that the change in slope related to higher injection pressure HRR profiles occurred earlier compared to the reference profiles because an increase in injection pressure allows better atomization of diesel injected leading to a better air-fuel mixing [28], the autoignition and the combustion occur earlier due to a shorter ignition delay (ID) [26]. HRR traces also show a long diffusive phase that overtakes the reference traces within CA50 range.

Figure 6 shows the effects of the fuel injection pressure in  $2000 \times 8$  test point. With higher diesel injection, the reference trend was replicated, except for 4 deg aTDC due to exceeding the noise and  $COV_{IMEP}$  limits. In this case, HRR profiles show more pronounced peaks, with an increase of about 2%/deg, because the rise of diesel injection pressure allowed better mixing of the charge and improved the first phase of the premixed combustion. It is also noticed that the diffusive phase of higher injection HRR profiles overlapped the reference ones.

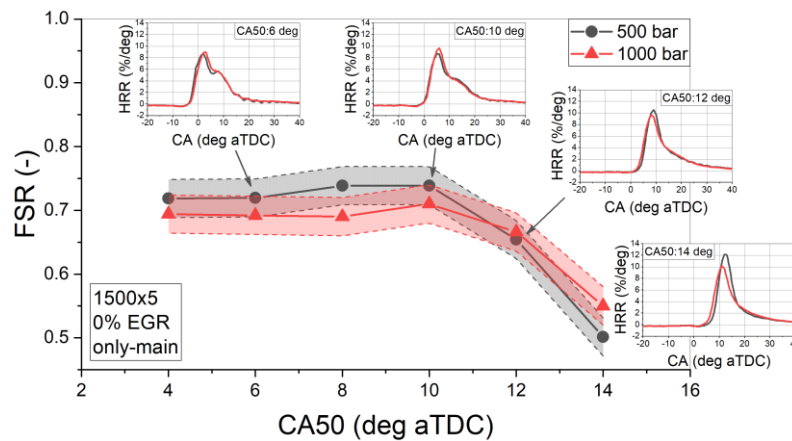


Figure 5. Effect of diesel injection pressure on FSR varying CA50 in 1500 × 5.

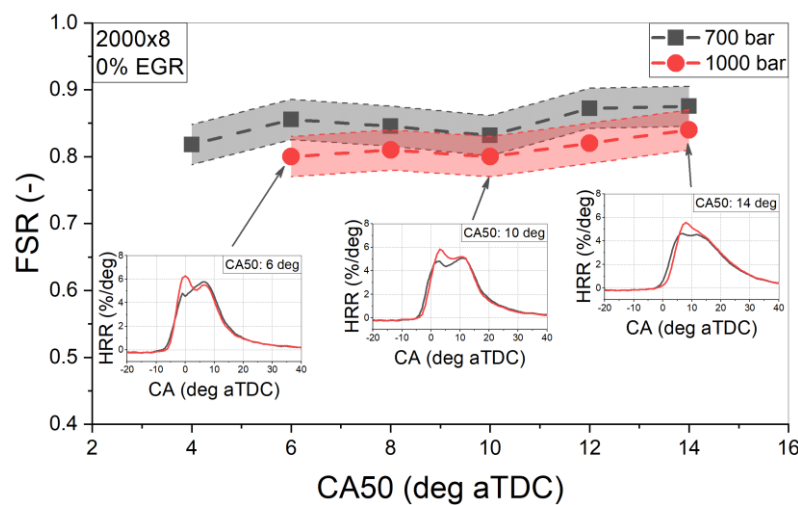
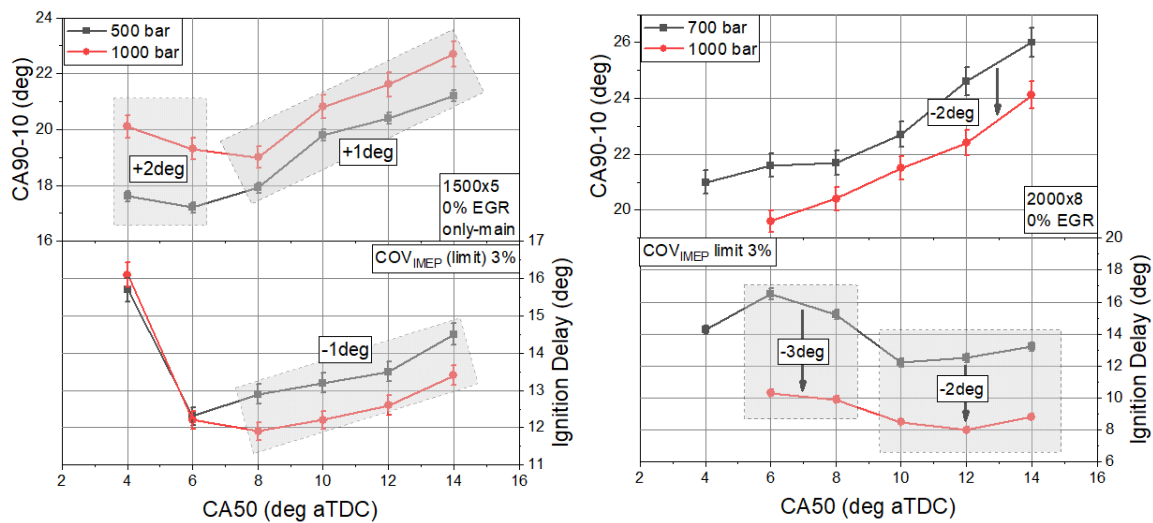


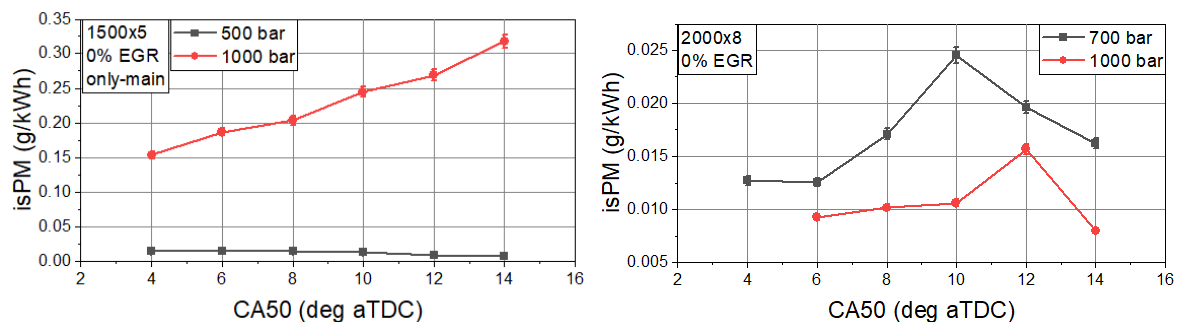
Figure 6. Effect of diesel injection pressure on FSR varying CA50 in 2000 × 8.

Figure 7 depicts the influence of injection pressure on combustion indicators for both test points in terms of CA10-90, ID. As seen, in 1500 × 5, the combustion duration rose due to the prolonged diffusive phase, as shown by the HRR profiles of Figure 5. It is reasonable because after the premixed phase, the remaining charge burned in the diffusion phase in a mixture of ethanol/air, which leads to a slower and prolonged combustion phase [29]. As already stated, with increasing injection pressure, the ignition delay decreased due to smaller particles of atomized fuel, which enhanced the mixing diesel and premixed mixture of ethanol-air hence ID shortened. On average, a shorter ID of about 1 deg CAD could be noticed. For higher loads (2000 × 8) a shorter combustion duration was observed, on average 2 deg less of the reference case. With the increase of the injection pressure and consequently a shorter ID, the greater fuel amount accumulated in the ID period leads to an increase in the premixed heat release [26], as the higher HRR peaks show in Figure 6. It is reasonable to assume more rapid combustion of the fuel mixture in the first part of the premixed combustion phase, consequently, shorter combustion duration was observed. Related to this point, retarding combustion phasing led to a rise of combustion duration from a minimum of 20 CAD to a maximum of 24 CAD.



**Figure 7.** Injection pressure effect on combustion duration and ID at  $1500 \times 5$  and  $2000 \times 8$  without EGR.

Figure 8 shows the rail pressure effect on PM, for both test points in the DF mode. The consistent reduction that can be observed between the trends comparison at  $2000 \times 8$  was mainly due to two reasons. First, as shown in Figure 6, a longer premixed phase allowed better PM oxidation. The locally available oxygen content was a key parameter to allow the PM oxidation during combustion process as also reported by Wagner et al. [30]. The use of oxygenated biofuels [31], like ethanol, combined with the high level of FSR achieved (Figure 6) led to less fuel-rich zones hence to a limited PM formation [32]. The prolonged diffusive phase, observed for  $1500 \times 5$  (Figure 5), and longer combustion duration (Figure 7), led to a worsening of the engine-out PM. As can be seen, its trend rose linearly from a minimum value of 0.15 g/kWh to a maximum of about 0.33 g/kWh. As shown in Figure 5 for lower values of FSR, higher values of PM were reached in the range 12–14 deg of CA50.



**Figure 8.** Influence of injection pressure on particulate matter (PM).

This section shows that the combined effect of higher injection pressure and a more complex injection pattern (related to  $2000 \times 8$ ) led to an improvement in terms of indicated PM emissions. For these reasons, in the following section, the evaluation with a multi injection strategy was also conducted for  $1500 \times 5$  test point.

### 3.3. Effects of Injection Pattern on FSR in the DF Mode

The effects of a multi-injection strategy, characterized by two pilot plus main injection pattern, as reported in Figure 2, in comparison with the reference one (only main) were evaluated. The investigation was conducted in the range 4–14 deg of CA50, at constant rail pressure (500 bar),  $SOI_{ethanol}$ , FSR and with no EGR to discriminate the injection pattern effect only. This analysis aimed to replicate the FSR values obtained with the only main and evaluate the effects on parameters.

Figure 9 shows the influence of the injection pattern of FSR varying CA50. The use of a multi-injection pattern led to reach the FSR limit imposed in the range 4–12 of CA50, while at 14 deg, the test point was not performed because misfire occurred. For more retarded combustion phasing, the mixture was below the lower flammability limit due to a too low in-cylinder temperature and an excess of air in the cylinder [19].

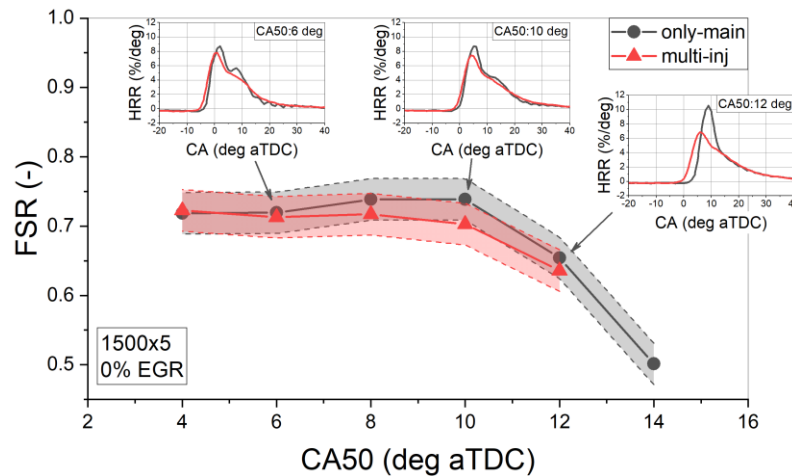


Figure 9. Effect of injection pattern on FSR function of CA50 in 1500 × 5.

The use of a single pulse strategy, as observed in Figure 9, led to an increase in the ignition delay, which allowed better air-fuels mixing with a more significant premixed phase [33]. These aspects justify a completely different HRR, in particular by delaying the combustion phasing [34]. The multi-injection strategy, as shown in Figure 9, guaranteed a reduction of the premixed phase, favoring the diffusive one, also assuring a significant decrease of the maximum rate of pressure rise and therefore of the combustion noise [35].

Figure 10 shows the influence of the injection pattern on the combustion indicators in terms of combustion noise and combustion efficiency. As expected, a general decrease of the combustion noise was observed, with a minimum difference of 4 dBA at 6 deg and a maximum reduction of 8 dBA (at 14 deg) retarding combustion phasing.

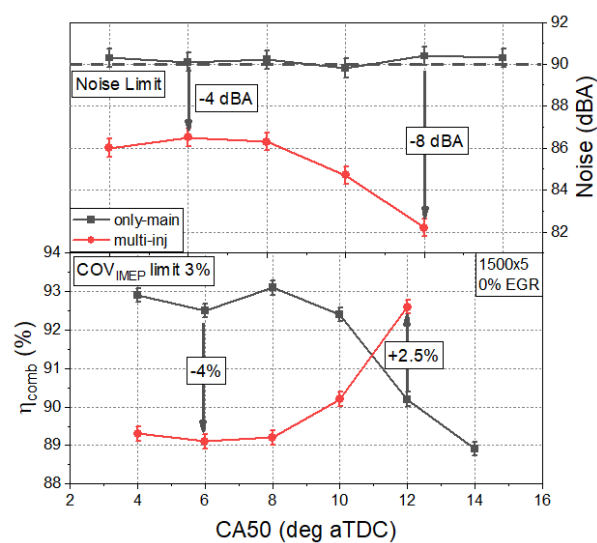


Figure 10. Influence of the injection pattern on combustion indicators.

A trend comparison of combustion efficiency is also depicted in Figure 10. A reduction for the multi-injection strategy is reasonably due to not full vaporization of the PFI ethanol that can lead to

ethanol impinging on the cylinder wall and combustion chamber [36] and incomplete combustion since an amount of mixture burns in the expansion stroke [37]. These aspects affect the combustion of the charge and consequently a worsening of HC and CO emissions, which can worsen the combustion efficiency if the diesel flame is extinguished before reaching the combustion chamber wall. For more retarded combustion phasing (12 deg aTDC), splitting the diesel injections helped to maintain higher mean in-cylinder temperature, which improved the oxidation of HC and CO emissions and consequently the combustion efficiency, as depicted in Figure 10.

No trend analysis was reported for specific indicated PM values due to their values lower than the minimum filter smoke number (FSN) relates to the resolution of smoke meter utilized during the experimental campaigns (Section 2.1). Despite different values, their order of magnitude is typical of a soot-less zone.

This section shows that the use of a multi-injection strategy also for the lower load case ( $1500 \times 5$ ) guaranteed the respect of FSR target and led to an improvement in terms of combustion noise and efficiency. For these reasons, the multi-injection strategy was also adopted for the subsequent experimental investigations related to  $1500 \times 5$  test point.

### 3.4. Effects of EGR on FSR in the DF Mode

This section analyzed the EGR influence on FSR and the combustion process in the DF mode. The evaluation was performed imposing typical Euro 6 engine-out NO<sub>x</sub> limit of 0.6 and 0.9 g/kWh for  $1500 \times 5$  and  $2000 \times 8$ , respectively. The goal was to reach the same FSR values obtained by the multi-injection strategy.

Figure 11 compares the FSR trends with and without EGR in  $1500 \times 5$  test point varying combustion phasing in the range 4–12 deg. For a more advanced CA50 (4 deg), the FSR value achieved was very low (0.2) due to the high thermal inertia of ethanol/diesel mixture using a high rate of EGR. Ethanol fraction was reduced to sustain the combustion. Retarding the combustion phasing FSR increased and its trend was closer to the reference point in the range 10–12 deg CA50.

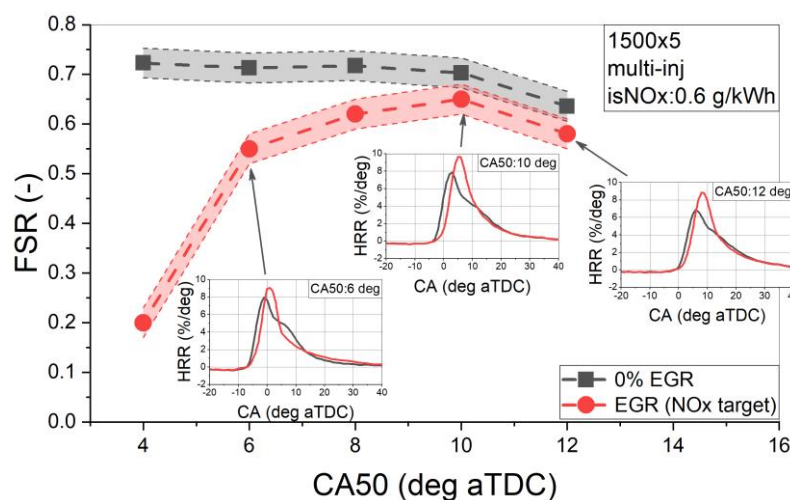


**Figure 11.** Effect of EGR on the FSR function of CA50 in  $1500 \times 5$  test point.

The combined effects of the use of EGR and the high heat of vaporization of ethanol allow a reduction of in-cylinder temperature and pressure [21] delaying the start of combustion. The dilution effect, when EGR was used, means a decreased oxygen concentration in the intake charge and less favorable thermodynamic conditions to initiate combustion. As a consequence, the combustion process was more premixed, producing a higher rate of heat release, and the trend became more obvious with increasing ethanol fraction [11]. The higher premixed combustion phase enhanced the in-cylinder mean temperature and accelerated the post-combustion of premixed diesel and alcohol fuel, and thus shortened the combustion duration [38].

Finally, it can be stated that, at the same engine speed-load, the combustion process, in terms of the HRR pattern, as shown in Figure 11, was similar within the CA50 range considered.

With an imposed limit of 0.9 g/kWh, in 2000 × 8 test point, over the CA50 range 6–12 deg, the fraction of ethanol injected was always lower than the reference one, as reported in Figure 12. As previously stated, delayed combustion was observed with a prominent premixed combustion phase, which affected noise, in an average of 1 dBA, in the whole CA50 range considered.

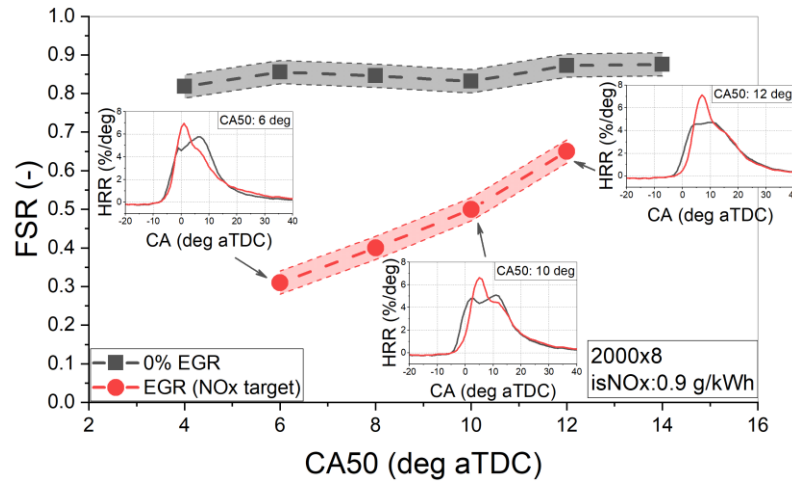


Figure 12. Effect of EGR on the FSR function of CA50 in 2000 × 8 test point.

Figure 13 shows the influence of EGR on combustion efficiency, and PM indicated specific emissions for both test points.

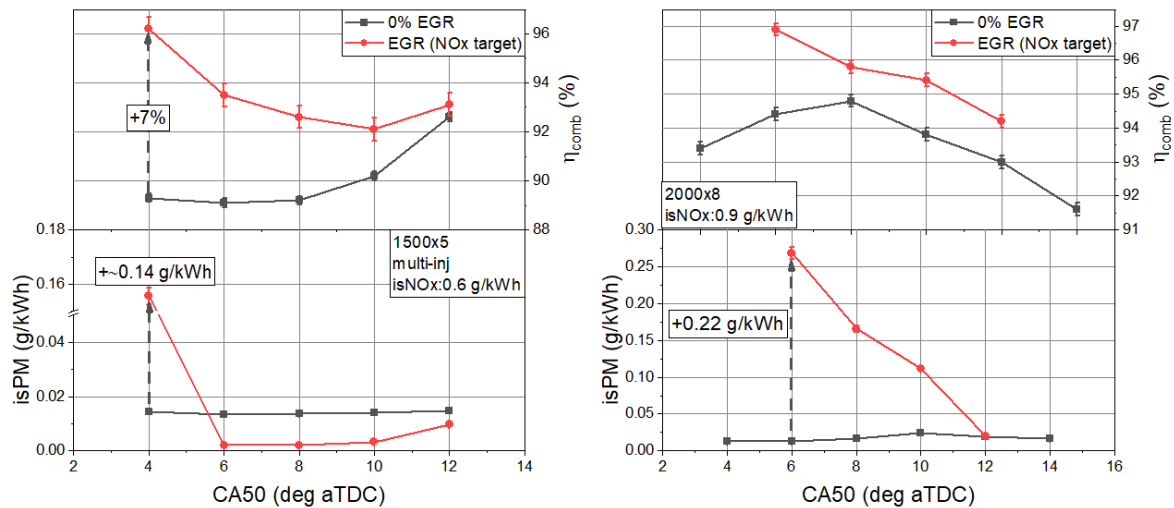


Figure 13. Influence of EGR on combustion efficiency and PM specific emissions.

For both test points, a general improvement of the combustion efficiency was observed within the CA50 range considered. It was reasonably due to a richer combustion process as lower air index ( $\lambda$ ) values shown in Figure 14.

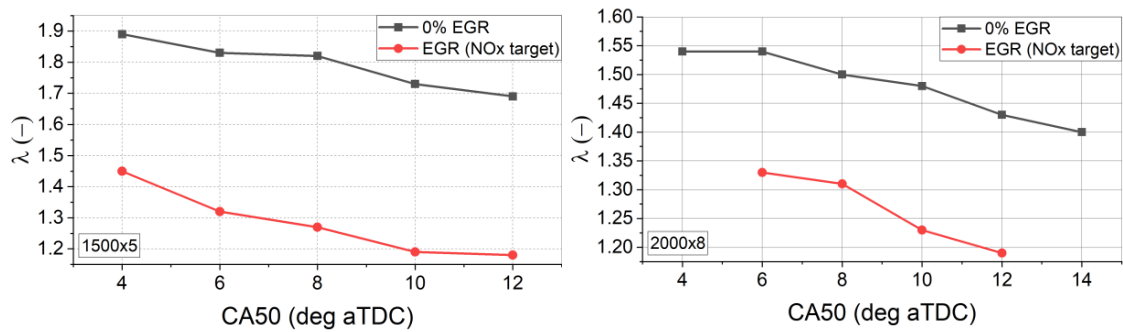


Figure 14. Air index with and without EGR: 1500  $\times$  5 and 2000  $\times$  8.

The ethanol addition could improve the PM reduction due to lower oxygen availability in the presence of EGR. As can be seen, the PM emission trend adopting EGR, at 1500  $\times$  5, was lower than the reference one except for an abrupt variation at 4 deg of CA50 due to the greater amount of diesel injected. For higher load, at 6 deg of CA50, the lower fraction of ethanol injected led to a PM penalty. Nevertheless, retarding combustion phasing the trend decreased due to the further FSR increment.

### 3.5. Effects of the Nozzle Hole Numbers on FSR in the DF Mode

This section aimed to cover the scientific gap in technical literature providing further information and discussion on the influence of the nozzle-hole number, 7 and 9, of the diesel injector on the maximum FSR reachable in the DF combustion mode and the GHG and PM emissions. All test conditions imposed in previous sections were kept constant to discriminate the nozzle effect.

Relating to the 9 nozzle-hole cases, in 1500  $\times$  5, the ethanol fraction increased retarding combustion phasing. On average, the FSR trend showed comparable values with the lower holes case in the range 6–10 deg of CA50, while at 4 and 12 deg higher values were reached as shown in Figure 15.

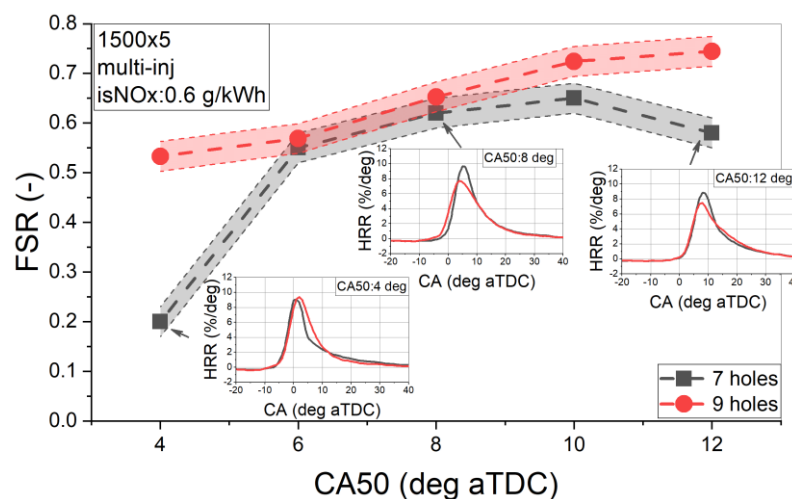
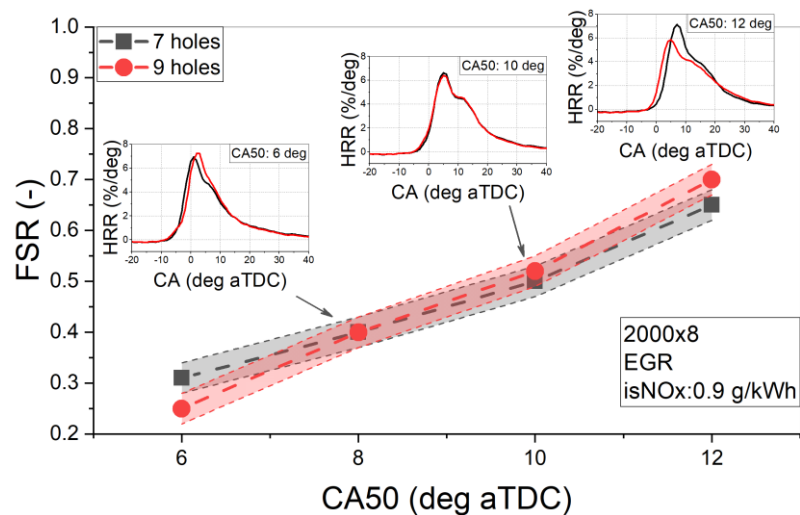


Figure 15. FSR function of CA50 in 1500  $\times$  5 test point, 9 holes vs. 7 holes.

The increasing of the nozzle holes diminished the reacting zone at a high temperature because of a more uniform distribution of the fuel and temperature, as confirmed in Lee et al. [39]. Therefore, retarding combustion phasing a reduction of temperature on average was expected, as the HRR profiles of 9 holes case shown in Figure 15.

For higher engine speed-load (2000  $\times$  8), instead, the FSR values were not influenced by a different nozzle hole number, as shown in Figure 16. A slight difference could be observed for more retarded combustion phasing. For both nozzle cases, the FSR trend increased retarding CA50.



**Figure 16.** FSR function of CA50 in 2000 × 8 test point, 9 holes vs. 7 holes.

In terms of the combustion process, no relevant difference could be noticed in the HRR pattern. An exception was at 12 deg where the combustion occurred earlier with a lower temperature premixed phase as shown by the lower HRR peak. Furthermore, a prominent diffusive phase could be observed.

The combustion characteristics related to different nozzle hole number are depicted in Figure 17. As can be seen, at lower load (5 bar BMEP) the 9 holes case showed the shortest combustion duration compared to the 7 holes case, with a maximum reduction of 5.5 deg at 4 deg aTDC and an average reduction of 2 deg retarding combustion phasing. In the DF combustion mode, when two fuels with different reactivity were involved in the combustion process, the combustion started in the high reactivity regions and gradually evolved towards low reactivity regions [40]. The increase in the nozzle hole number led to a reduction of the orifice diameter and, since it had the same hydraulic flow rate, an improvement of fuel atomization hence a better mixing of the charge. The formation of a higher reactivity zone in the combustion chamber and the more atomized fuel allowed shorter combustion duration. The charge cooling effect of the ethanol fraction combined with well mixed air-fuel led to an increase of ID.

Shorter combustion duration was also observed for the higher load case. A discrepancy was found at 12 deg of CA50. In this case, due to lower mean temperature and a prolonged diffusive phase, as shown in Figure 16, increased combustion duration was observed. In the range 6–10 deg, the lower value of FSR shortened the ID.

At a lower load, the 9-hole nozzle shows an improvement in the combustion noise compared to the 7-hole one with values aligned with the conventional diesel mode. In 2000 × 8, for both nozzles tested, the effect of ethanol was more predominant, probably due to the higher injection pressures. Insensitivity to combustion noise was observed, resulting in higher values than the conventional target, in the range of 6–7 dBA in the entire CA50 range considered.

Figure 18 shows the effect of holes numbers on thermal and combustion efficiency, indicated specific PM, and CO<sub>2</sub> emissions.

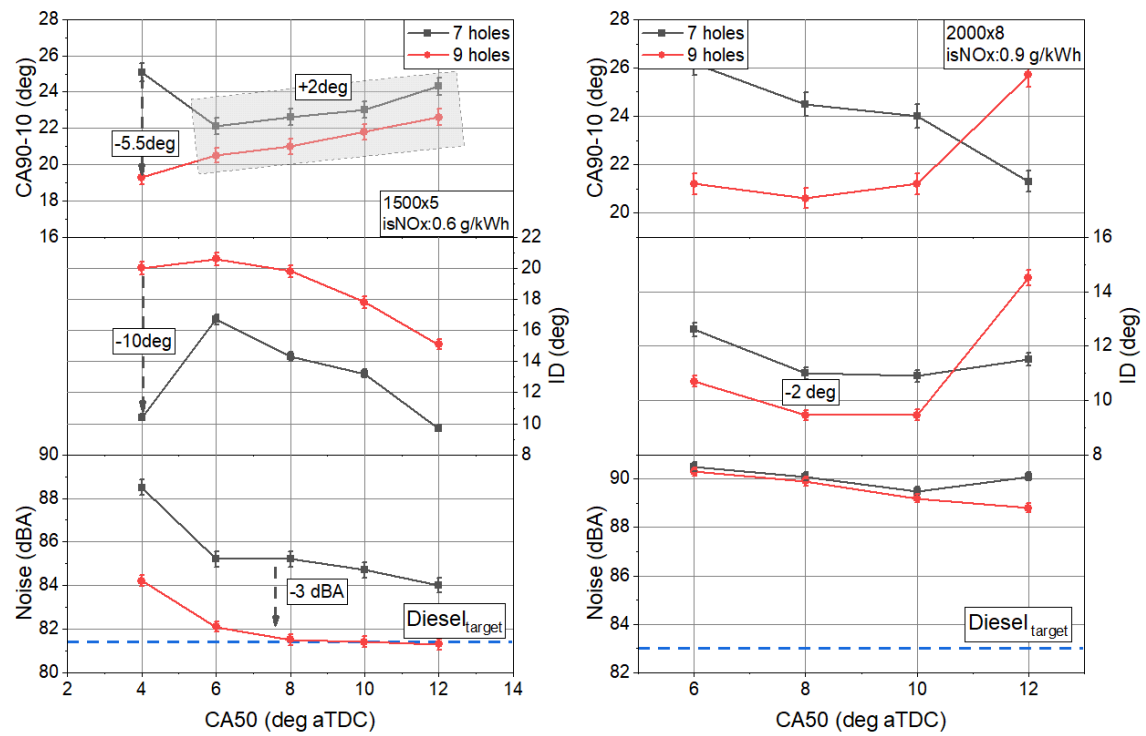


**Figure 17.** Effect of a different nozzle hole number on CA90-10, ID, COV<sub>IMEP</sub> and combustion noise.

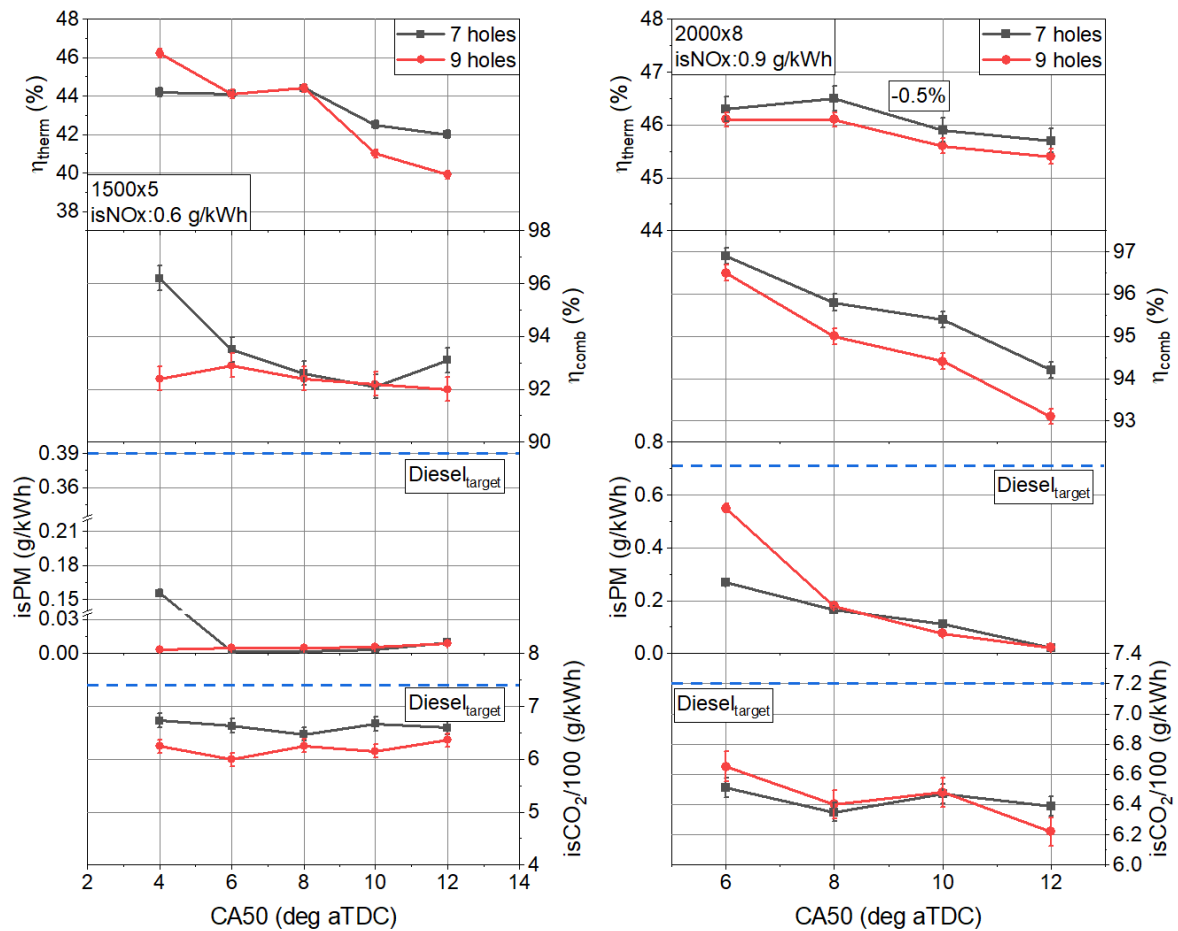


**Figure 18.** Influence of a different nozzle hole number on efficiencies, PM and CO<sub>2</sub> indicated specific emissions.

The different nozzle hole number, for  $1500 \times 5$ , had no influence on the indicated specific PM except for more advanced combustion phasing (4 deg) related to fewer nozzle cases. The abrupt variation observed was due to the lower value of FSR achieved, as shown in Figure 15. For higher load and speed, PM decreased while increasing the ethanol fraction for both nozzle cases. Figure 18 compares engine-out PM emissions between DF and conventional diesel modes. The ethanol addition significantly reduced them in both cases investigated, in particular at 5 bar of BMEP. These benefits were evident by adopting a high FSR because of the reduced quantity of diesel fuel, which reacted with the ethanol–air mixture leading to dominant premixed combustion, with a consequent reduction of PM, in this case of about 95% in the CA50 range considered. An exception at the lowest CA50, for both, tested points, where a lower FSR justified an important difference in terms of soot, of about 90% and 50%, for  $1500 \times 5$  and  $2000 \times 8$ , respectively.

No relevant influence could be noticed in both cases for thermal efficiency, while the combustion efficiency decrease was related to the CO/HC trend. Related to this point, further explanations are given below.

The effect of different nozzle hole numbers on indicated specific CO and HC emissions are illustrated in Figure 19. As can be seen for both test points, the adoption of 9 holes injector led to an increase of HC emissions retarding combustion phasing. The trend was mainly evident at  $2000 \times 8$ . With more jets, since the same hydraulic flow rate, the amount of diesel per zone in the combustion chamber was lower. So, retarding combustion phasing the unburned fraction increased owing to lower mean in-cylinder temperature, as lower peaks of HRR shown in Figure 15. Despite the HC worsening, the combustion efficiency, as shown in Figure 18, maintained acceptable values within the CA50 range considered.

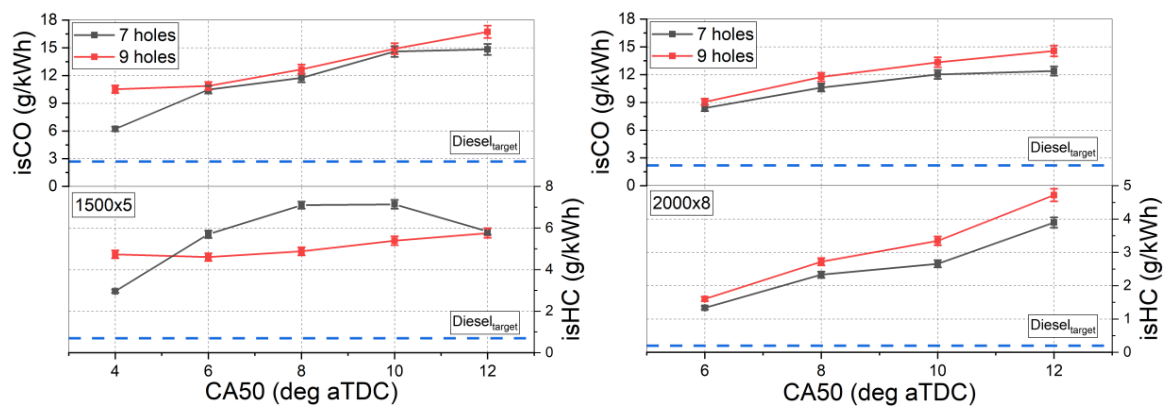


Figure 19. Influence of the different nozzle hole number on indicated CO and HC.

For both test points, the CO emissions increased with further increment of ethanol fraction injected, but CO levels decreased increasing the engine load. The high heat of vaporization of ethanol (Table 2) and the consequent cooling effect on the charge reasonably affected the CO oxidation. The CO<sub>2</sub> emissions (Figure 18) strongly depended on CO oxidation. In  $1500 \times 5$ , the lower mean in-cylinder temperature due to higher FSR reached (Figure 15), did not allow complete oxidation of CO and a lower level of CO<sub>2</sub> emitted could be observed in the whole operating range observed. For a higher load, no relevant differences comparing the CO<sub>2</sub> trend could be noticed due to an improved combustion process and the higher values of combustion efficiency compared with the lower load case are shown in Figure 18.

In all cases, as remarked in Figure 19, the ethanol fumigation increased the CO and HC emissions owing to the cooling effect of the ethanol on the combustion process. For both test points, it was also found that the CO<sub>2</sub> emissions were lower compared to the diesel target due to the lower C/H ratio and the worsening of the fuel oxidation to produce CO<sub>2</sub>.

It is worth highlighting that the multi-injection pattern used in this analysis was calibrated for 7 holes case. Reasonably, for 9 holes case, a dedicated calibration can reveal further improvements not visible at this stage.

#### 4. Conclusions

In this study, an experimental investigation was carried out to assess the influence on the maximum ethanol fraction and combustion behavior of typical calibration parameters (rail pressure, injection pattern and EGR) and the geometrical parameter (nozzle holes number) employing ethanol in the DF combustion mode. All the tests were performed, with imposed limits on combustion noise and  $COV_{IMEP}$ . The main outcomes can be summarized as follows:

- At lower loads, higher injection pressures, up to 1000 bar, and multiple injection strategies did not influence the maximum FSR rate significantly. On the contrary, at higher loads, a multiple injection pattern and higher injection pressure led to a higher FSR value, up to 0.8.
- With EGR, a reduction of the maximum FSR was observed in both test points. For lower loads, the lowest ethanol fraction (FSR equal to 0.2) was reached for more advanced combustion phasing. By retarding the CA50 an increasing trend was observed with FSR values until up to 0.65. Similar FSR values were reached at higher loads for retarded combustion phasing.
- The ethanol addition was generally very effective in terms of PM reduction due to the high FSR values achieved, and we expect an abrupt variation to be obtained for more advanced combustion phasing. For higher loads, despite the decreasing trend of PM emission, a higher specific value could be observed, and in the range of 0.03–0.25 g/kWh, compared to the no EGR case.
- A higher number of nozzle holes allowed us to reach higher FSR at lower loads, and over the whole area of investigation. Conversely, for higher loads, no influence on FSR was observed. In this case, despite the HC worsening, the combustion efficiency maintained acceptable values within the CA50 range considered. At lower load, the 9-hole nozzle shows an improvement in combustion noise, 3 dBA on average, and a reduction of the combustion duration compared to the 7-hole. Increasing the load insensitivity to a different hole number was observed. In terms of engine-out PM emissions, no relevant differences could be drawn by adopting a different nozzle hole number. The effect of ethanol addition on PM reduction was more predominant rather than the effect of nozzle holes. At lower loads, the 9 hole case showed lower  $CO_2$  emissions compared to the 7 one. For a higher load, no relevant differences in  $CO_2$  emissions could be noticed.

Based on the above results, it can be stated that the use of ethanol in the dual-fuel mode led to a consistent decrease of engine-out PM and  $CO_2$  emissions compared to the diesel one. These benefits were obtained at the cost of higher emissions of HC and CO, but this worsening might be acceptable due to lower PM tendency and to lower carbon nature of the ethanol. Moreover, with the same diesel quantity injected, it was suggested to use lower nozzle hole numbers to reduce the HC emission. The near-zero PM emissions, especially for lower load case, suggested further experimental investigations with a different nozzle hole number to evaluate the effects of a greater amount of direct fuel that can be injected.

#### Highlights

- Ethanol in CI engines as a GHG and PM emissions enabler.
- Maximum fuel substitution ratio and GHG and PM emissions by increasing the injection of the nozzle hole number injector were analyzed.
- Improved atomization by increasing the hole injector led to a higher ethanol fraction injected, allowing for the reduction of GHG and PM emissions.
- Significant reduction of PM and  $CO_2$  in the dual-fuel combustion mode.

**Author Contributions:** Data curation, R.I.; performed the experiments, R.I. and M.S.; methodology, G.D.B.; supervision, I.D., C.B. and G.D.B.; writing—original draft, G.D.L. All authors have read and agreed to the published version of the manuscript.

**Funding:** This research received no external funding.

**Conflicts of Interest:** The authors declare no conflict of interest.

## Nomenclature

aTDC	after top dead centre
BMEP	brake mean effective pressure
CA	crank angle
CA50	combustion phasing
CA90-10	combustion duration
CDC	conventional diesel combustion
CI	compression ignition
CO	carbon monoxide
CO <sub>2</sub>	carbon dioxide
COV <sub>IMEP</sub>	IMEP coefficient of variation
DF	dual fuel
EGR	exhaust gas recirculation
GHG	greenhouse gas
$\eta_{comb}$	combustion efficiency
$\eta_{th}$	thermodynamic efficiency
FSN	filter smoke number
FSR	fuel substitution ratio
HC	hydrocarbon
HRR	heat release rate
ID	ignition delay
ISx	indicated specific emission
IMEP	indicated mean effective pressure
LD	light-duty
LHV <sub>d</sub>	low heating value of directly injected fuel
LHV <sub>p</sub>	low heating value of premixed fuel
LTC	low temperature combustion
NO <sub>x</sub>	nitrogen oxides
PFI	port fuel injection
PM	particulate matter
PRR	pressure rise rate
SCE	single cylinder engine
SOI	start of injection
SOI <sub>diesel</sub>	start of injection diesel
SOI <sub>Ethanol</sub>	start of injection ethanol

## References

1. U.S. Energy Information Administration. International Energy Outlook 2019. Available online: <https://www.eia.gov/outlooks/ieo/pdf/ieo2019.pdf> (accessed on 14 August 2020).
2. Heywood, J.B. *Internal Combustion Engine Fundamentals*; McGraw-Hill: New York, NY, USA, 1988.
3. CO<sub>2</sub> Engine Performance Standards for Cars and Vans (2020 Onwards). Available online: [https://ec.europa.eu/clima/policies/transport/vehicles/regulation\\_en](https://ec.europa.eu/clima/policies/transport/vehicles/regulation_en) (accessed on 10 August 2020).
4. Ayodhya, A.S.; Narayanappa, K.G. An overview of after-treatment systems for diesel engines. *Environ. Sci. Pollut. Res.* **2018**, *25*, 35034–35047. [CrossRef] [PubMed]
5. Pidol, L.; Lecointe, B.; Starck, L.; Jeuland, N. Ethanol-biodiesel-Diesel fuel blends: Performances and emissions in conventional Diesel and Low Temperature Combustions. *Fuel* **2012**, *93*, 329–338. [CrossRef]

6. Krishnamoorthi, M.; Malayalamurthi, R.; He, Z.; Kandasamy, S. A review on low temperature combustion engines: Performance, combustion and emission characteristics. *Renew. Sustain. Energy Rev.* **2019**, *116*, 109404. [\[CrossRef\]](#)
7. Divekar, P.S.; Asad, U.; Tjong, J.; Chen, X.; Zheng, M. An engine cycle analysis of diesel-ignited ethanol low-temperature combustion. *Proc. Inst. Mech. Eng. Part D J. Automob. Eng.* **2015**, *230*, 1057–1073. [\[CrossRef\]](#)
8. Divekar, P.S.; Asad, U.; Tjong, J.; Chen, X.; Zheng, M. Experimental and numerical study on different dual-fuel combustion modes fuelled with gasoline and diesel. *Appl. Energy* **2014**, *113*, 722–733. [\[CrossRef\]](#)
9. Heuser, B.; Kremer, F.; Pischinger, S.; Rohs, H.; Holderbaum, B.; Körfer, T. An Experimental Investigation of Dual-Fuel Combustion in a Light Duty Diesel Engine by in-Cylinder Blending Ethanol and Diesel. *SAE Int. J. Engines* **2016**, *9*, 11–25. [\[CrossRef\]](#)
10. Ianniello, R.; Di Blasio, G.; Marialto, R.; Beatrice, C.; Cardone, M. Assessment of Direct Injected Liquefied Petroleum Gas-Diesel Blends for Ultra-Low Soot Combustion Engine Application. *Appl. Sci.* **2020**, *10*, 4949. [\[CrossRef\]](#)
11. Di Blasio, G.; Beatrice, C.; Molina, S. *Effect of Port Injected Ethanol on Combustion Characteristics in a Dual-Fuel Light Duty Diesel Engine*; No. 2013-01-1692; SAE Technical Paper: Troy, MI, USA, 2013. [\[CrossRef\]](#)
12. Çelebi, Y.; Aydın, H. An overview on the light alcohol fuels in diesel engine. *Fuel* **2019**, *236*, 890–911. [\[CrossRef\]](#)
13. Kim, E.J.; Kim, S.; Choi, H.G.; Han, S.J. Co-production of biodiesel and bioethanol using psychrophilic microalga *Chlamydomonas* sp. KNM0029C isolated from Arctic sea ice. *Biotechnol. Biofuels* **2020**, *13*, 20. [\[CrossRef\]](#)
14. Szybist, J.P.; Song, J.; Alam, M.; Boehman, A.L. Biodiesel combustion, emissions and emission control. *Fuel Process. Technol.* **2007**, *88*, 679–691. [\[CrossRef\]](#)
15. Serrà, A.; Artal, R.; García-Amorós, J.; Gómez, E.; Philippe, L. Circular zero-residue process using microalgae for efficient water decontamination, biofuel production, and carbon dioxide fixation. *Chem. Eng. J.* **2020**, *388*, 124278. [\[CrossRef\]](#)
16. Coulier, J.; Verhelst, S. Using Alcohol Fuels in Dual Fuel Operation of Compression Ignition Engines: A Review. In Proceedings of the 28th CIMAC World Congress Congress on Combustion Engine, Helsinki, Finland, 6–10 June 2016; pp. 1–12.
17. Damyanov, A.; Hofmann, P.; Geringer, B.; Schwaiger, N.; Pichler, T.; Siebenhofer, M. Biogenous ethers: Production and operation in a diesel engine. *Automot. Engine Technol.* **2018**, *3*, 69–82. [\[CrossRef\]](#)
18. Abu-Qudais, M.; Haddad, O.; Qudaisat, M. The effect of alcohol fumigation on diesel engine performance and emissions. *Energy Convers. Manag.* **2000**, *41*, 389–399. [\[CrossRef\]](#)
19. Wang, Q.; Wei, L.; Pan, W.; Yao, C. Investigation of operating range in a methanol fumigated diesel engine. *Fuel* **2015**, *140*, 164–170. [\[CrossRef\]](#)
20. Imran, A.; Varman, M.; Masjuki, H.H.; Kalam, M.A. Review on alcohol fumigation on diesel engine: A viable alternative dual fuel technology for satisfactory engine performance and reduction of environment concerning emission. *Renew. Sustainable Energy Rev.* **2013**, *26*, 739–751. [\[CrossRef\]](#)
21. Pedrozo, V.B.; May, I.; Zhao, H. Exploring the mid-load potential of ethanol-diesel dual-fuel combustion with and without EGR. *Appl. Energy* **2017**, *193*, 263–275. [\[CrossRef\]](#)
22. Asad, U.; Zheng, M.; Tjong, J. Experimental Investigation of Diesel-Ethanol Premixed Pilot-Assisted Combustion (PPAC) in High Compression Ratio Engine. *Sae Int. J. Engines* **2016**, *9*, 1059–1071. [\[CrossRef\]](#)
23. Beatrice, C.; Di Blasio, G.; Pesce, F.C.; Vassallo, A.; Avolio, G.; Ianniello, R. Key Fuel Injection System Features for Efficiency Improvement in Future Diesel Passenger Cars. *Sae Int. J. Adv. Curr. Pr. Mobil.* **2019**, *1*, 1084–1099. [\[CrossRef\]](#)
24. National Center for Biotechnology Information, PubChem Compound Database; CID=887. Available online: <https://pubchem.ncbi.nlm.nih.gov/compound/887> (accessed on 10 August 2020).
25. Belgiorio, G.; Boscolo, A.; Dileo, G.; Numidi, F.; Pesce, F.C.; Vassallo, A.; Ianniello, R.; Beatrice, C.; Di Blasio, G. *Experimental Study of Additive-Manufacturing-Enabled Innovative Diesel Combustion Bowl Features for Achieving Ultra-Low Emissions and High Efficiency*; SAE Technical Paper 2020-37-0003; SAE International in United States: Troy, MI, USA, 2020. [\[CrossRef\]](#)
26. Canakci, M.; Sayin, C.; Ozsezen, A.N.; Turkcan, A. Effect of Injection Pressure on the Combustion, Performance, and Emission Characteristics of a Diesel Engine Fueled with Methanol-blended Diesel. *Fuel Energy Fuels* **2009**, *23*, 2908–2920. [\[CrossRef\]](#)

27. Tutak, W.; Lukacs, K.; Szwaja, S.; Bereczky, A. Alcohol–diesel fuel combustion in the compression ignition engine. *Fuel* **2015**, *154*, 196–206. [\[CrossRef\]](#)
28. Tschoeke, H.; Graf, A.; Stein, J.; Krußger, M.; Schaller, J.; Breuer, N.; Engeljehring, K.; Schindler, W. Diesel Engine Exhaust Emissions. In *Handbook of Diesel Engine*; Springer: Berlin, Germany, 2010; pp. 417–485.
29. Tsang, K.S.; Zhang, Z.H.; Cheung, C.S.; Chan, T.L. Reducing emissions of a diesel engine using fumigation ethanol and a diesel oxidation catalyst. *Energy Fuels* **2010**, *24*, 6156–6165. [\[CrossRef\]](#)
30. Wagner, U.; Eckert, P.; Spicher, U. Possibilities of Simultaneous In-Cylinder Reduction of Soot and NO<sub>x</sub> Emissions for Diesel Engines with Direct Injection. *Int. J. Rotating Mach.* **2008**, *2008*, 175956. [\[CrossRef\]](#)
31. Dijkstra, R.; Di Blasio, G.; Boot, M.; Beatrice, C.; Bertoli, C. *Assessment of the Effect of Low Cetane Number Fuels on a Light Duty CI Engine: Preliminary Experimental Characterisation in PCCI Operating Condition*; SAE paper 2011-24-0053; SAE International: Troy, MI, USA, 2011. [\[CrossRef\]](#)
32. Damyanov, A.; Hofmann, P. Operation of a diesel engine with intake manifold alcohol injection. *Automot. Engine Technol.* **2019**, *4*, 17–28. [\[CrossRef\]](#)
33. Shamun, S.; Belgiorno, G.; Di Blasio, G. Engine Parameters Assessment for Alcohols Fuels Application in Compression Ignition Engine. In *Alternative Fuels and Their Utilisation Strategies in Internal Combustion Engines*; Springer: Singapore, 2020.
34. Busch, S.; Zha, K.; Miles, P.C. Investigations of closely coupled pilot and main injections as a means to reduce combustion noise in a small-bore direct injection Diesel engine. *Int. J. Engine Res.* **2015**, *16*, 13–22. [\[CrossRef\]](#)
35. Selim, M.Y. Effect of exhaust gas recirculation on some combustion characteristics of dual fuel engine. *Energy Convers. Manag.* **2003**, *44*, 707–721. [\[CrossRef\]](#)
36. Surawski, N.C.; Ristovski, Z.D.; Brown, R.J.; Situ, R. Gaseous and particle emissions from an ethanol fumigated compression ignition engine. *Energy Convers. Manag.* **2012**, *54*, 145–151. [\[CrossRef\]](#)
37. Knight, B.; Bittle, J.; Jacobs, T. Efficiency Consideration of Later-Phased Low Temperature Diesel Combustion. In Proceedings of the ASME, Internal Combustion Engine Division Fall Technical Conference, ICEF2018-9657, San Antonio, TX, USA, 12–15 September 2010. [\[CrossRef\]](#)
38. Lu, H.; Yao, A.; Yao, C.; Chen, C.; Wang, B. An investigation on the characteristics of and influence factors for NO<sub>2</sub> formation in diesel/methanol dual fuel engine. *Fuel* **2019**, *235*, 617–626. [\[CrossRef\]](#)
39. Lee, B.H.; Song, J.H.; Chang, Y.J.; Jeon, C.H. Effect of the number of fuel injector holes on characteristics of combustion and emissions in a diesel engine. *Int. J. Automot. Technol.* **2010**, *11*, 783–791. [\[CrossRef\]](#)
40. Dong, S.; Yang, C.; Ou, B.; Lu, H.; Cheng, X. Experimental investigation on the effects of nozzle-hole number on combustion and emission characteristics of ethanol/diesel dual-fuel engine. *Fuel* **2018**, *217*, 1–10. [\[CrossRef\]](#)

**Publisher’s Note:** MDPI stays neutral with regard to jurisdictional claims in published maps and institutional affiliations.



© 2020 by the authors. Licensee MDPI, Basel, Switzerland. This article is an open access article distributed under the terms and conditions of the Creative Commons Attribution (CC BY) license (<http://creativecommons.org/licenses/by/4.0/>).